Smidt MH, Stroink H, Bruinenberg JFM, Peeters M (2004). Encephalopathy associated with influenza A. *Eur J Paediatr Neurol* **8:** 257–260.

Stolp H, Dziegielewska K, Ek C, Habgood M, Lane M, Potter A, Saunders N (2005). Breakdown of the blood-brain barrier to proteins in white matter of the developing brain following systemic inflammation. *Cell Tissue Res* **320:** 369–378.

Togashi T, Matsuzono Y, Narita M, Morishima T (2004). Influenza-associated acute encephalopathy in Japanese children in 1994–2002. *Virus Res* **103:** 75–78.

Toovey S (2008). Influenza-associated central nervous system dysfunction: a literature review. *Travel Med Infect Dis* **6:** 114–124.

Tsuda Y, Isoda N, Sakoda Y, Kida H (2009). Factors responsible for plaque formation of A/duck/Siberia/272/1998 (H13N6) influenza virus on MDCK cells. *Virus Res* **140:** 194–198.

Yao D, Chen Y, Kuwajima M, Shiota M, Kido H (2004). Accumulation of mini-plasmin in the cerebral capillaries causes vascular invasion of the murine brain by a pneumotropic influenza A virus: implications for influenza-associated encephalopathy. *Biol Chem* **385:** 487–492.

Yokota S, Imagawa T, Miyamae T, Ito S, Nakajima S, Nezu A, Mori M (2000). Hypothetical pathophysiology of acute encephalopathy and encephalitis related to influenza virus infection and hypothermia therapy. *Pediatr Int* **42:** 197–203.

This paper was first published online on Early Online on 29 March 2010.

J Med Primatol doi:10.1111/j.1600-0684.2009.00395.x

ORIGINAL ARTICLE

Amelioration of pneumonia with *Streptococcus pneumoniae* infection by inoculation with a vaccine against highly pathogenic avian influenza virus in a non-human primate mixed infection model

Taichiro Miyake[1,2], Kosuke Soda[3], Yasushi Itoh[1], Yoshihiro Sakoda[3], Hirohito Ishigaki[1], Tomoya Nagata[1,4], Hideaki Ishida[1], Misako Nakayama[1], Hiroichi Ozaki[5], Hideaki Tsuchiya[6], Ryuzo Torii[6], Hiroshi Kida[3,7] & Kazumasa Ogasawara[1]

1 Department of Pathology, Shiga University of Medical Science, Otsu, Shiga, Japan
2 Department of Ophthalmology, Shiga University of Medical Science, Otsu, Shiga, Japan
3 Department of Disease Control, Graduate School of Veterinary Medicine, Hokkaido University, Sapporo, Japan
4 Department of Otorhinolaryngology, Head and Neck Surgery, Shiga University of Medical Science, Otsu, Shiga, Japan
5 Faculty of Agriculture, Tottori University, Tottori, Japan
6 Research Center for Animal Life Science, Shiga University of Medical Science, Otsu, Shiga, Japan
7 Research Center for Zoonosis Control, Hokkaido University, Sapporo, Japan

Keywords
cynomolgus macaque – H7N7 – superinfection

Correspondence
Yasushi Itoh, Department of Pathology, Shiga University of Medical Science, 485 Setatsukinowa, Otsu, Shiga 520-2192, Japan.
Tel.: +81 77 548 2172;
fax: +81 77 548 2423;
e-mail: yasushii@belle.shiga-med.ac.jp

Accepted October 9, 2009.

Abstract

Background Highly pathogenic avian influenza virus (HPAIV) infection has a high mortality rate in humans. Secondary bacterial pneumonia with HPAIV infection has not been reported in human patients, whereas seasonal influenza viruses sometimes enhance bacterial pneumonia, resulting in substantial morbidity and mortality. Therefore, if HPAIV infection were accompanied by bacterial infection, an increase in mortality would be expected. We examined whether a vaccine against HPAIV prevents severe morbidity caused by mixed infection with HPAIV and bacteria.
Methods H7N7 subtype of HPAIV and *Streptococcus pneumoniae* were inoculated into cynomolgus macaques with or without vaccination of inactivated whole virus particles.
Results Vaccination against H7N7 HPAIV decreased morbidity caused by HPAIV and pneumonia caused by *S. pneumoniae*. Bacterial replication in lungs was decreased by vaccination against HPAIV, although the reduction in bacterial colonies was not significant.
Conclusions Vaccination against HPAIV reduces pneumonia caused by bacterial superinfection and may improve prognosis of HPAIV-infected patients.

Introduction

Influenza virus and *Streptococcus pneumoniae* are the two pathogens that cause the majority of respiratory infections in humans. Influenza virus infection results in pneumonitis in which lymphocytes infiltrate into lung interstices, whereas bacteria induce pneumonia in which neutrophils infiltrate into lung alveoli. Although influenza virus infection alone results in pneumonitis, secondary bacterial pneumonia may be a major cause of substantial morbidity and mortality during typical influenza pandemics, including the major pandemic of 1918–1919 [2, 21]. Although bacterial pneumonia has not been reported in patients infected with H5N1 or H7N7 highly pathogenic avian influenza virus (HPAIV) [5, 26], the possibility of mortality being increased by

mixed infection with HPAIV and bacteria has not been ruled out. Thus, it seems reasonable to assume that the prevention of influenza virus replication will improve bacterial pneumonia in case of mixed infection, resulting in decreased morbidity and mortality; however, this assumption has not been examined, at least in macaque models. In this study, as HPAIV A/chicken/Netherlands/2586/2003 (H7N7) (NL2586) was more pathogenic, i.e. duration of high fever and loss of appetite, in cynomolgus macaques than A/Vietnam/1194/2004 (H5N1) [8] (Itoh, Y., *et al.*, unpublished data), we examined the efficacy of inoculation with a vaccine against H7N7 HPAIV for ameliorating bacterial pneumonia in a non-human primate model with mixed infection.

In recent years, results of epidemiological and animal model studies have demonstrated that initial respiratory tract infection alters immunity to a second unrelated pathogen, even long after the resolution of the first pathogen and in the absence of cross-reactive immunity [15, 29]. Several factors have been proposed to be involved in this altered immunity, including suppression of neutrophil function [1, 4, 13] and induction of inhibitory interleukin (IL)-10 [27, 28]. In another study, it was shown that interferon-γ produced by T cells in the lung after viral infection inhibits alveolar macrophage-mediated microbial clearance and, consequently, leads to enhanced susceptibility to secondary bacterial infection [24].

We previously demonstrated that whole virus particle vaccines inactivated by formalin induced protective immune responses, including antibody and cytotoxic T lymphocyte responses, against HPAIV in mice [18]. We selected vaccine strains of non-pathogenic H5N1 and H7N7 viruses, A/duck/Hokkaido/Vac-1/2004 (Vac-1) and A/duck/Hokkaido/Vac-2/2004 (Vac-2) respectively, from a virus library containing 144 different combinations of 16 hemagglutinin (HA) and 9 neuraminidase (NA) subtypes of non-pathogenic viruses [10] and produced whole virus particle vaccines as described previously [17, 20]. Then, we examined immune responses induced by subcutaneous inoculation with the whole virus particle vaccine and protective efficiency against H5N1 and H7N7 HPAIVs in non-human primate models [8] (Itoh, Y., *et al.*, unpublished data). The whole virus particle vaccines ameliorated morbidity including high fever and appetite loss in cynomolgus macaques. HPAIV was detected in samples from unvaccinated macaques for 5–7 days after challenge with HPAIV, whereas HPAIV was recovered from samples of the vaccinated macaques only for 1–2 days after challenge.

In the present study, vaccination with Vac-2 against H7N7 HPAIV decreased histopathological pneumonia caused by *S. pneumoniae* in macaques simultaneously infected with H7N7 HPAIV and *S. pneumoniae*. Bacterial growth in the lung was diminished by vaccination with Vac-2, although the reduction was not significant. Therefore, development of vaccines against influenza virus might be crucial for preventing high rates of morbidity and mortality in pandemics.

Materials and methods

Viruses

Non-pathogenic influenza virus A/duck/Hokkaido/Vac-2/2004 (H7N7) (Vac-2, National Center for Biotechnology Information taxonomy database ID: 390987) is a genetic reassortant generated by co-infection with A/duck/Mongolia/736/2002 (H7N7) and A/duck/Hokkaido/49/1998 (H9N2) in chicken embryos. PB2, PB1, PA, HA, NA and NS genes of Vac-2 were derived from the H7N7 virus, and NP and M genes were derived from the H9N2 virus [17]. HPAIV A/chicken/Netherlands/2586/2003 (H7N7) (NL2586, National Center for Biotechnology Information taxonomy database ID: 533037) was provided by Dr Ilaria Capua [L'Office International des Épizooties (OIE), Food and Agriculture Organization of the United Nations (FAO), and National Reference Laboratory for Newcastle Disease and Avian Influenza, Istituto Zooprofilattico Sperimentale delle Venezie, Italy]. The percent sequence similarity between Vac-2 and NL2586 was 97% in HA and 98% in NA at the amino acid level. The viruses were propagated in the allantoic cavities of 10-day-old embryonated hen's eggs at 35°C for 48 hours. For an inactivated vaccine, the infectious allantoic fluids were concentrated and purified by high-speed centrifugation through a 10–50% sucrose density gradient (112,500 *g* for 90 minutes) and then treated with 0.1% formalin at 4°C for 1 week. The purified viruses were then suspended in PBS. Inactivation of the viruses was confirmed by the absence of detectable hemagglutination following inoculation of the materials into 10-day-old embryonated hen's eggs after one passage [20]. The amount of whole particle vaccines was indicated as that of entire protein including HA and the other viral proteins. The vaccine used in this study contained 42,667 HA units of HA antigen in 1 mg vaccine.

For virus titration, serial dilutions of swabs and whole blood samples were inoculated onto confluent Madin–Darby canine kidney (MDCK) cells. The MDCK cells were then cultured in MEM including 0.1% BSA. Cytopathic effects were examined with a microscope 72 hours later, and mean tissue infectious dose ($TCID_{50}$)/ml was calculated [8].

Bacteria

Streptococcus pneumoniae was obtained from Dr Takayuki Ezaki (Gifu University, GTC261, NCTC7465). The bacteria were stored at −80°C in 10% (w/v) skimmed milk. For preparation of the animal inoculation, 10-μl aliquots of bacteria were removed from frozen stock and inoculated into 40 ml of brain–heart infusion broth (Becton, Dickinson and Company, Sparks, MD, USA) and then incubated at 37°C for 17 hours. Bacteria were collected by centrifugation at 700 *g* for 30 minutes and resuspended in 10 ml saline. A 1-ml aliquot of the saline suspension was used for inoculation into each animal, and the remainder was used for quantification and colony counting by serial dilution [16, 19].

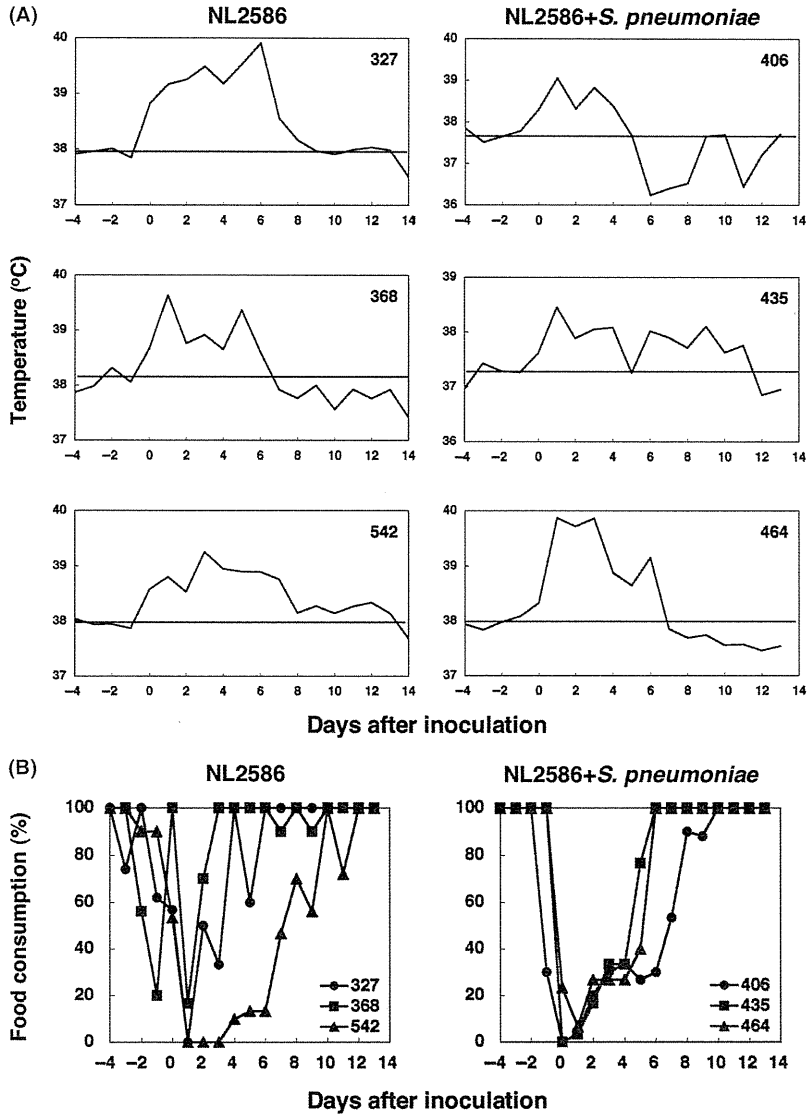

Fig. 1 Body temperatures and food consumption of macaques after inoculation of H7N7 HPAIV (NL2586) with or without *Streptococcus pneumoniae*. NL2586 (4×10^7 $TCID_{50}$) was inoculated onto conjunctivas and into nasal cavities and tracheas with *S. pneumoniae* (1.2×10^9 CFU) into tracheas of cynomolgus macaques (Nos 406, 435 and 464). The other macaques (Nos 327, 368 and 542) were inoculated with NL2586 (4×10^7 $TCID_{50}$) onto conjunctivas and into nasal cavities and tracheas. (A) Body temperatures were monitored by telemetry transmitters implanted in the peritoneal cavities. Average temperatures of the highest and lowest temperatures on one day are time-dependently shown. Lines drawn horizontally indicate the average temperature levels at pre-infection. (B) Appetite was reflected by the amount of food consumed, which was calculated from the numbers of residual and fed pellets.

J Med Primatol **39** (2010) 58–70

Swab samples were collected as described in the following. To count the colony number, swab samples were serially diluted. Diluted fluid was cultured on blood agar plates with 5% sheep blood (Eiken Chemical Co. Ltd, Tokyo, Japan) at 37°C for 21 hours. *Streptococcus pneumoniae* colonies were identified by their hemolytic activity and counted. *Streptococcus pneumoniae* colonies characteristically produce a zone of alpha hemolysis (incomplete, green) on blood agar [16].

Animals

Five- to seven-year-old cynomolgus macaques (*Macaca fascicularis*) from Vietnam were used with permission of the Shiga University of Medical Science Animal Experiment Committee and Biosafety Committee and in accordance with Guidelines for the Husbandry and Management of Laboratory Animals of Research Center for Animal Life Science at Shiga University of Medical Science. In the text and figures, individual macaques are distinguished by identification numbers. The absence of H7N7-specific antibody in the sera was confirmed before experiments using antigen-specific enzyme-linked immunosorbent assays (ELISA). Under anesthesia 2 weeks before virus inoculation, telemetry probes (TA10CTA-D70; Data Sciences International, St Paul, MN, USA) to monitor body temperature were implanted in the macaques' peritoneal cavities. The macaques used in this study did not carry B virus, hepatitis E virus, *Mycobacterium tuberculosis*, *Shigella* spp., *Salmonella* spp. or *Entamoeba histolytica* [8].

The vaccines (1 mg/dose) were inoculated subcutaneously with syringes with alum (500 μl; Superfos Biosector, Vaerloese, Denmark) twice with a 2-week interval between injections. Saline (500 μl) was injected into control animals. Five weeks after the second vaccination, NL2586 (4×10^7 $TCID_{50}$) was inoculated on conjunctivas (1×10^6 $TCID_{50}$/50 μl for each eye) and

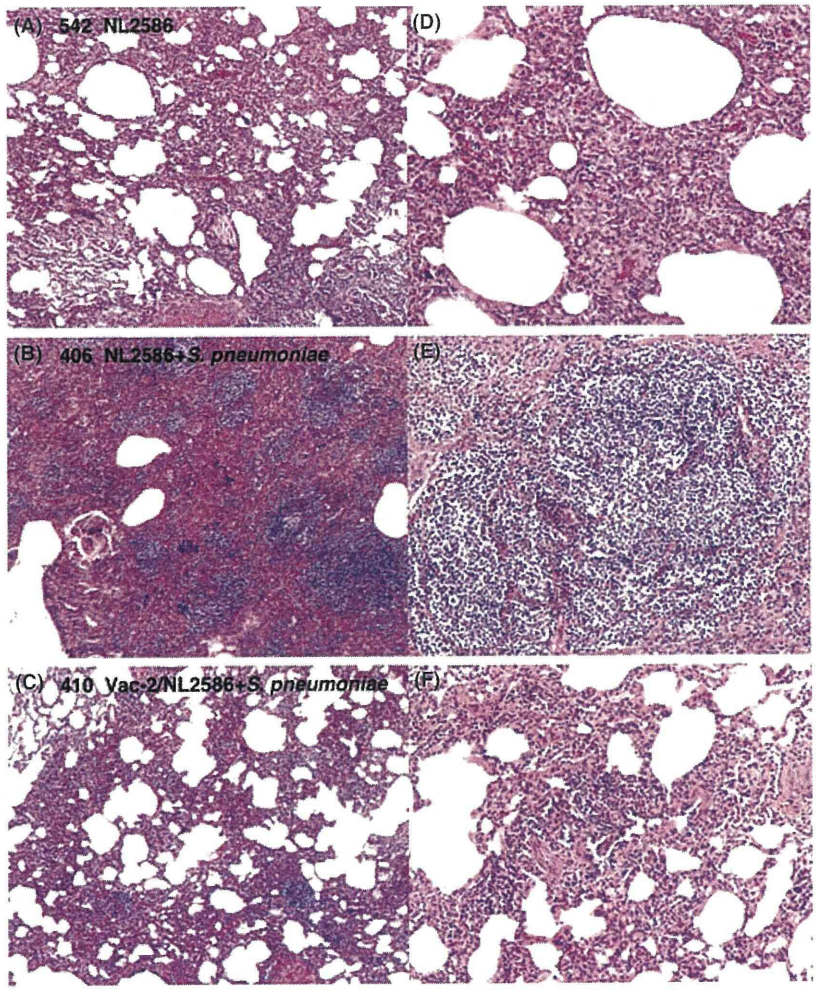

Fig. 2 Lung histology of cynomolgus macaques inoculated with NL2586 with or without *Streptococcus pneumoniae*. Cynomolgus macaques were subcutaneously vaccinated with inactivated whole particles of Vac-2 twice. Seven weeks after the first vaccination (5 weeks after the second vaccination), the macaques were inoculated with pathogens. After autopsy (i.e. 14 days after the challenge), the lungs were fixed in 10% formalin. Hematoxylin and eosin (H&E) staining was conducted as described in Materials and methods. The figures (A–C) show the low power magnification and (D–F) high power magnification. (A, D) An unvaccinated macaque (No. 542) inoculated with NL2586 alone; (B, E) an unvaccinated macaque (No. 406) inoculated with NL2586 and *S. pneumoniae*; (C, F) a vaccinated macaque (No. 410) inoculated with NL2586 and *S. pneumoniae*.

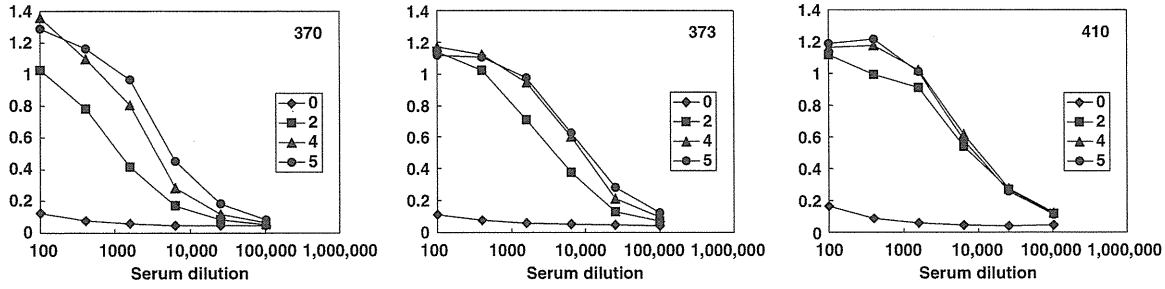

Fig. 3 Antibody responses specific for H7N7 vaccine antigens in cynomolgus macaques immunized with whole virus particle vaccines. Cynomolgus macaques were subcutaneously inoculated with whole virus particle vaccines of Vac-2 (1 mg/dose) with alum twice with a 2-week interval between injections. Sera were collected before (0 week) and after vaccination (2, 4 and 5 weeks after the first vaccination). IgG antibodies specific for Vac-2 antigens in sera were analyzed at indicated dilutions using ELISA. Optical densities at 450 nm are shown.

into nasal cavities (9×10^6 $TCID_{50}$/450 μl for each nasal cavity) with pipettes and into tracheas (2×10^7 $TCID_{50}$/1 ml) with catheters. *Streptococcus pneumoniae* (1.2×10^9 CFU/1 ml) was inoculated into tracheas with catheters. Experiments using NL2586 were performed in the biosafety level 3 facility of the Research Center for Animal Life Science, Shiga University of Medical Science.

Under anesthesia, two cotton sticks were used to collect each swab; subsequently, the sticks were immersed in 1 ml of PBS containing 0.1% BSA. A bronchoscope (MEV-2560; Machida Endoscope Co., Ltd, Tokyo, Japan) and brushes (BC-203D-2006; Olympus, Tokyo, Japan) were used to collect samples of bronchi [25]. The brushes were immersed in 1 ml of PBS containing BSA.

Histological examination

After autopsy, the lungs were fixed in 10% formalin for at least 1 week. Hematoxylin and eosin staining was conducted as previously described [8].

Enzyme-linked immunosorbent assays

The antibody titers of serum samples against Vac-2 antigens were determined using ELISA. Then 96-well plates were coated with 50 μl of purified Vac-2 (20 μg/ml) [8]. For analysis of antibody responses against *S. pneumoniae*, *S. pneumoniae* was cultured as described previously. Thereafter, *S. pneumoniae* was suspended in PBS and inactivated by heat (100°C, 10 minutes). ELISA plates were coated with 50 μl of inactivated *S. pneumoniae* (2×10^5 CFU) [22]. Serially diluted samples were incubated overnight in the coated plates. After washing five times, horseradish peroxidase-conjugated anti-monkey IgG antibody (MP Biomedicals, Inc./Cappel, Aurora, OH, USA) (1:1000 × 50 μl) was added and incubated for 1 hour at room temperature. Horseradish peroxidase activity was assessed using 3, 3′, 5, 5′-tetramethyl benzidine substrate (100 μl). The reaction was stopped by the addition of 1 M hydrogen chloride (100 μl). Optical density was measured at 450 nm.

For detection of IL-10, a monkey IL-10 ELISA kit was used as according to a manufacturer's instruction (Bender MedSystems GmbH, Vienna, Austria). IL-10 secretion was expressed as relative changes comparing with IL-10 production after infection and before infection.

Virus neutralization assay

The serum samples were pretreated with receptor destroying enzyme (RDEII; Denka Seiken, Tokyo, Japan) at 37°C overnight and then inactivated at 56°C for 1 hour. Diluted samples were mixed with 50 $TCID_{50}$ of NL2586 for 1 hour. Then the mixture was added onto an MDCK monolayer. After 1-h incubation, the suspension was removed, and the cells were cultured in MEM containing 0.1% BSA. After incubation at 35°C for 3 days, the number of wells with cytopathic effects was counted in quadruplicate culture. Neutralization titers were expressed as the dilution in which cytopathic effects were observed in 50% of the wells.

Results

Pathogenicity of simultaneous infection with H7N7 HPAIV and Streptococcus pneumoniae in cynomolgus macaques and efficacy of ameliorating pneumonia with Streptococcus pneumoniae by a vaccine against H7N7 HPAIV

H7N7 HPAIV NL2586 (4×10^7 $TCID_{50}$) or both NL2586 and *S. pneumoniae* were inoculated on conjunctivas and in nasal cavities and tracheas of cynomolgus

J Med Primatol **39** (2010) 58–70

Table 1 *Streptococcus pneumoniae* titers in bronchial swabs

		Number of colonies (×10^2 CFU/ml)								
	Animal (dpi)	0	1	2	3	4	5	6	7	8
Without Vac-2	406	0	0	0	0	0	0	0	0	0
	435	0	1	33	2	0	0	0	0	0
	464	0	0	0	0	1	0	0	0	0
With Vac-2	370	0	0	0	0	0	0	0	0	0
	373	0	0	0	0	0	0	0	0	0
	410	0	0	0	0	0	0	0	0	0

Macaques were subcutaneously vaccinated with Vac-2 twice. Five weeks after the second vaccination, the macaques were inoculated with NL2586 and *S. pneumoniae*. Bronchial swabs were collected with a bronchoscope on the indicated days. dpi, days post inoculation with NL2586 and *S. pneumoniae*.

macaques. The body temperature was time-dependently expressed by an average of highest and lowest temperatures on 1 day, and the body temperature after the virus challenge was compared with that before the virus challenge. After NL2586 inoculation, higher body temperature than that before the challenge was observed for 6–13 days in the macaques (Nos 327, 368, 542; Fig. 1A, left panels). After simultaneous inoculation with NL2586 and *S. pneumoniae*, high body temperature was observed until day 4 (No. 406, followed by unstable low temperature until day 12), day 6 (No. 464) and day 11 (No. 435) (Fig. 1A, right panels).

After NL2586 challenge, loss of appetite was observed in two macaques for 2–5 days and in one macaque for 10 days, and after challenge with both NL2586 and *S. pneumoniae*, loss of appetite was observed in two macaques for 6 days and in one macaque for 10 days (Fig. 1B). We also compared weight loss among macaques challenged with the pathogens. All of the macaques had lost weight on day 14 after the virus challenge; the average weight ratio (after/before the challenge) in macaques challenged with NL2586 alone was 90%, whereas that in macaques challenged with NL2586 and *S. pneumoniae* was 88%. These were not significantly different and coincide with the findings for appetite loss ($P = 0.33$).

Next, we performed histological examination of the lungs 14 days after the challenge. The lungs of macaques infected with NL2586 alone indicated interstitial lymphocyte infiltration in thick alveolar walls (pneumonitis) (Fig. 2A,D), whereas pneumonitis and alveolar lymphocyte infiltration with a few neutrophils

Table 2 *Streptococcus pneumoniae* titers in lungs at autopsy

	Number of colonies (×10^2 CFU/ml)					
	Without Vac-2			With Vac-2		
Lung lobe	406	435	464	370	373	410
Upper right	0	1	5	0	4	1
Middle right	0	13	3	1	1	3
Lower right	0	0	6	4	1	2
Upper left	1	0	5	0	0	2
Middle left	0	2	1	1	1	1
Lower left	0	1	1	0	0	2
Total	1	17	21	6	7	11

Lung tissues were collected at autopsy (14 days after inoculation with NL2586 and *S. pneumoniae*). Tissues were homogenized and suspended in PBS to be adjusted to 10% (w/v) solution.

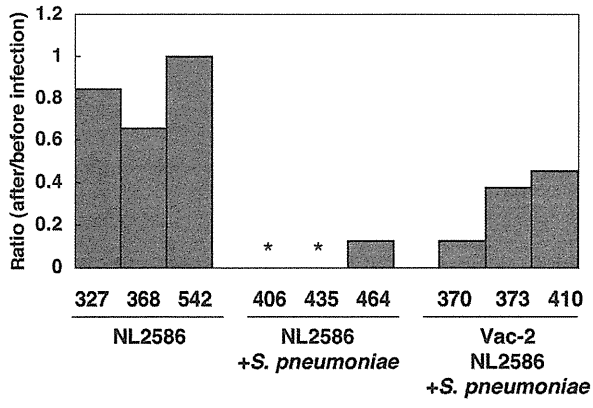

Fig. 4 IL-10 secretions in nasal swab samples. The levels of IL-10 in the samples were analyzed by ELISA. Nasal swabs were collected on day 0 before inoculation and day 8 after inoculation with NL2586 with or without *Streptococcus pneumoniae* as described in Table 3. The levels on day 8 were compared with the day 0 baseline to determine the relative changes in each macaque. Average fold-changes of IL-10 (day 8/day 0) are 0.83, 0.04 and 0.32 in macaques inoculated with NL2586 alone, unvaccinated macaques inoculated with NL2586 and *S. pneumoniae*, and vaccinated macaques inoculated with NL2586 and *S. pneumoniae* respectively, when the concentrations below the detection limit were calculated as 0 unit/ml (*). The differences of IL-10 relative levels are significant in NL2586 alone vs. NL2586 and *S. pneumoniae* ($P = 0.002$) and in NL2586 alone vs. Vac-2 + NL2586 and *S. pneumoniae* ($P = 0.02$).

(pneumonia) was observed in lungs of macaques infected with both NL2586 and *S. pneumoniae* (Fig. 2B,E). It was likely that acute-phase inflammation with neutrophils against *S. pneumoniae* disappeared following lymphocyte infiltration (i.e. tissue-repairing phase) 2 weeks after the simultaneous infection.

The above findings indicated that simultaneous infection resulted in histopathological pneumonitis and pneumonia but did not result in enhanced morbidity in the macaques. Thus, we histologically examined the efficacy of a vaccine, Vac-2, against H7N7 HPAIV for improving the bacterial pneumonia. Macaques were subcutaneously immunized twice with inactivated Vac-2, and subsequent increase in vaccine antigen-specific IgG in sera was confirmed (Fig. 3). Five weeks after the second vaccination, NL2586 and *S. pneumoniae* were inoculated into the macaques. Fourteen days after the challenge, lung tissue was examined at autopsy. The lungs of vaccinated macaques showed slight pneumonitis, but only weak pneumonia was seen in the lungs even after infection with both NL2586 and *S. pneumoniae* (Fig. 2C,F). Thus, we concluded that the vaccine against H7N7 HPAIV prevented severe bacterial pneumonia.

Bacterial growth in the bronchi and lungs of cynomolgus macaques infected with NL2586

We also examined bacterial growth in the bronchi and lungs of macaques simultaneously infected with NL2586 and *S. pneumoniae*. Bacterial colonies were detected in the bronchi of macaques 435 and 464 until day 4 after inoculation (Table 1), whereas bacterial colonies were observed in the lungs of all three macaques on day 14 (Table 2). On the other hand, bacterial colonies were decreased in the lungs of vaccinated macaques compared with those in the non-vaccinated macaques, although the reduction was not significant ($P = 0.47$) (Table 2). In addition, no bacterial colony was detected in the bronchi of vaccinated macaques, whereas a few bacterial colonies were detected in the bronchi of non-vaccinated macaques (Table 1). These findings are compatible with the histological severity.

We analyzed IL-10 production after the infection as it has been reported that IL-10 controlled lung inflammation during influenza virus infection [23, 28]. IL-10 production in nasal swab samples from macaques infected with NL2586 alone was not altered on day 8 after the infection comparing with that before the infection, whereas IL-10 production after the inoculation with NL2586 and *S. pneumoniae* was significantly decreased in macaques with and without vaccination ($P = 0.002$ in NL2586 alone vs. NL2586 + *S. pneumoniae*, $P = 0.02$ in NL2586 alone and Vac-2 + NL2586 + *S. pneumoniae*; Fig. 4). However, vaccinated macaques infected with HPAIV and *S. pneumoniae* showed intermediate IL-10 reduction because of low bacterial growth in the vaccinated macaques (Tables 1 and 2). These findings suggest that *S. pneumoniae* infection suppress IL-10 production in macaques and that low production of IL-10 may enhance inflammation in the lung of unvaccinated macaques as observed in histological results (Fig. 2).

Virus replication in swab samples from cynomolgus macaques after challenge with NL2586 or both NL2586 and Streptococcus pneumoniae

We examined virus replication in nasal swab samples from cynomolgus macaques after challenge with

Table 3 Virus recovery from nasal swabs of macaques inoculated with NL2586

		Virus titer [log 10 ($TCID_{50}$/ml)]									
Inoculation	Animal[1] (dpi)	1	2	3	4	5	6	7	8	10	12
NL2586	327	3.50	3.67	3.00	5.33	3.50	2.67	<	<	<	<
	368	2.67	2.33	2.00	2.23	<	<*	<	<	<	<
	542	<*	<	<*	1.67	1.67	2.50	<	<	<	<
NL2586	406	4.23	2.00	2.50	<*	<	<*	<*	<	<	<
+*S. pneumoniae*	435	3.50	3.00	2.50	2.00	2.50	3.00	<*	<*	<	<
	464	3.33	1.50	2.67	2.50	<*	<*	<	<	<	<
Vac-2	370	2.33	2.33	<	<	<	<	<	<	<	<
NL2586	373	<*	<	<	<	<	<	<	<	<	<
+*S. pneumoniae*	410	<	<	<	<	<	<	<	<	<	<

dpi, days post infection.

The symbol '<' indicates that the virus titer was less than the detection limit (<10 $TCID_{50}$/ml).

The symbol '<*' indicates that one cytopathic effect-positive well was observed in quadruplicate culture of undiluted sample solution.

[1]Each macaque was inoculated with NL2586 (4×10^7 $TCID_{50}$) and/or *S. pneumoniae* (1.2×10^9 CFU) on day 0.

J Med Primatol **39** (2010) 58–70

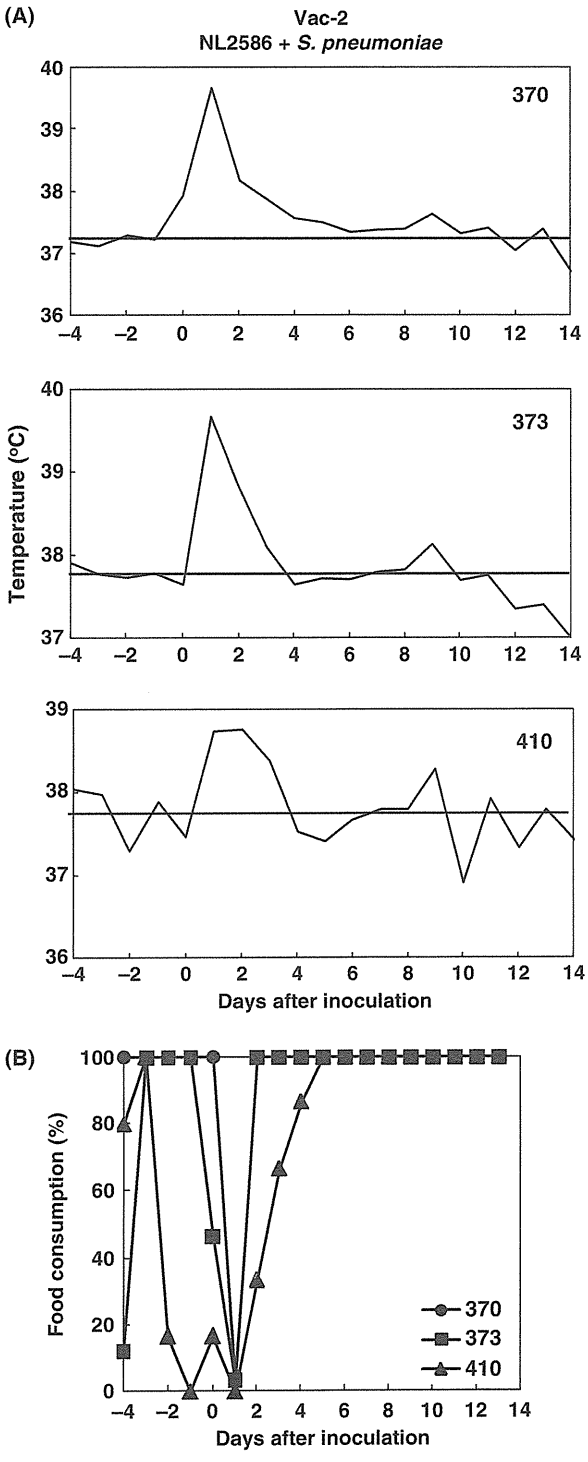

Fig. 5 Body temperatures and food consumption of vaccinated macaques after inoculation of H7N7 HPAIV (NL2586) with *Streptococcus pneumoniae*. Cynomolgus macaques (Nos 370, 373 and 410) were subcutaneously vaccinated twice. Seven weeks after the first vaccination (5 weeks after the second vaccination), NL2586 (4×10^7 $TCID_{50}$) was inoculated onto conjunctivas and into nasal cavities and tracheas with *S. pneumoniae* (1.2×10^9 CFU) into tracheas. (A) Body temperatures were monitored by telemetry transmitters implanted in the peritoneal cavities. Average temperatures of the highest and lowest temperatures on one day are time-dependently shown. Lines drawn horizontally indicate the average temperature levels at pre-infection. (B) Appetite was reflected by the amount of food consumed, which was calculated from the numbers of residual and fed pellets.

NL2586 or both NL2586 and *S. pneumoniae*. The virus was detected in nasal swab samples from the macaques until day 6 after inoculation with NL2586 (average 6 days; Table 3). Similarly, after simultaneous infection with NL2586 and *S. pneumoniae*, the virus was detected in nasal swab samples from the macaques until days 6–8 after the challenge (average 7 days, $P = 0.16$ vs. NL2586 alone). On the other hand, in swab samples from the vaccinated macaques, the virus was detected until day 2 after simultaneous challenge with NL2586 and *S. pneumoniae* (average 1 day, $P = 0.002$ vs. without vaccination). Therefore, it was clearly shown that pre-inoculation with whole particles of Vac-2 decreased H7N7 HPAIV replication in the respiratory tract after simultaneous infection with H7N7 HPAIV and *S. pneumoniae*. In addition, the average weight of vaccinated macaques on day 14 after challenge was 92% of the weight on day 0. Therefore, loss of weight was significantly reduced by vaccination ($P = 0.025$, vs. 88% in unvaccinated macaques as stated above). Furthermore, the average duration of abnormal body temperature after inoculation with NL2586 and *S. pneumoniae* was 2.67 days in vaccinated macaques (Fig. 5A) but 10.67 days in unvaccinated macaques (Fig. 1A) ($P = 0.01$). The average duration of appetite loss was 2.67 days in vaccinated macaques (Fig. 5B) but 7.33 days in unvaccinated macaques (Fig. 1B), although the difference was not statistically significant ($P = 0.06$). Thus, prevention of viral replication by the vaccine would decrease bacterial growth, severity of bacterial pneumonia and morbidity of infection.

Immune responses against HPAIV affected by mixed infection with Streptococcus pneumoniae

We examined immune responses against H7N7 virus and *S. pneumoniae* after infection to see whether mixed infection altered responses against the pathogens. As it was technically difficult to prepare purified antigen of NL2586 for ELISA, we used Vac-2 antigen to examine antibody responses against H7N7 virus. Serum IgG

responses specific for Vac-2 antigen in the unvaccinated macaques were elevated on day 8 after infection with NL2586 alone (Fig. 6, left panels) and the levels on day 14 were higher than those on day 8. IgG responses specific for the Vac-2 in sera from the unvaccinated macaques infected with NL2586 and *S. pneumoniae* were comparable to those from the macaques infected with NL2586 alone (Fig. 6, middle panels). Recall IgG responses in the vaccinated macaques were observed on day 8 after the infection as the antibody responses on day 8 had rapidly increased to the similar level on day 14 (Fig. 6, right panels). Infection with *S. pneumoniae* did not affect IgG responses against H7N7 virus. This finding was also seen in a neutralization assay against NL2586 (Table 4): no difference in neutralization activities of sera between macaques infected with NL2586 alone and macaques infected with NL2586 and *S. pneumoniae* was observed.

Next, we examined IgG responses against *S. pneumoniae* (Fig. 7). Two of the three unvaccinated macaques (Nos 435 and 464) showed IgG specific responses against *S. pneumoniae* after inoculation with NL2586 and *S. pneumoniae*, and one macaque (No. 406) showed very weak IgG responses against *S. pneumo-*

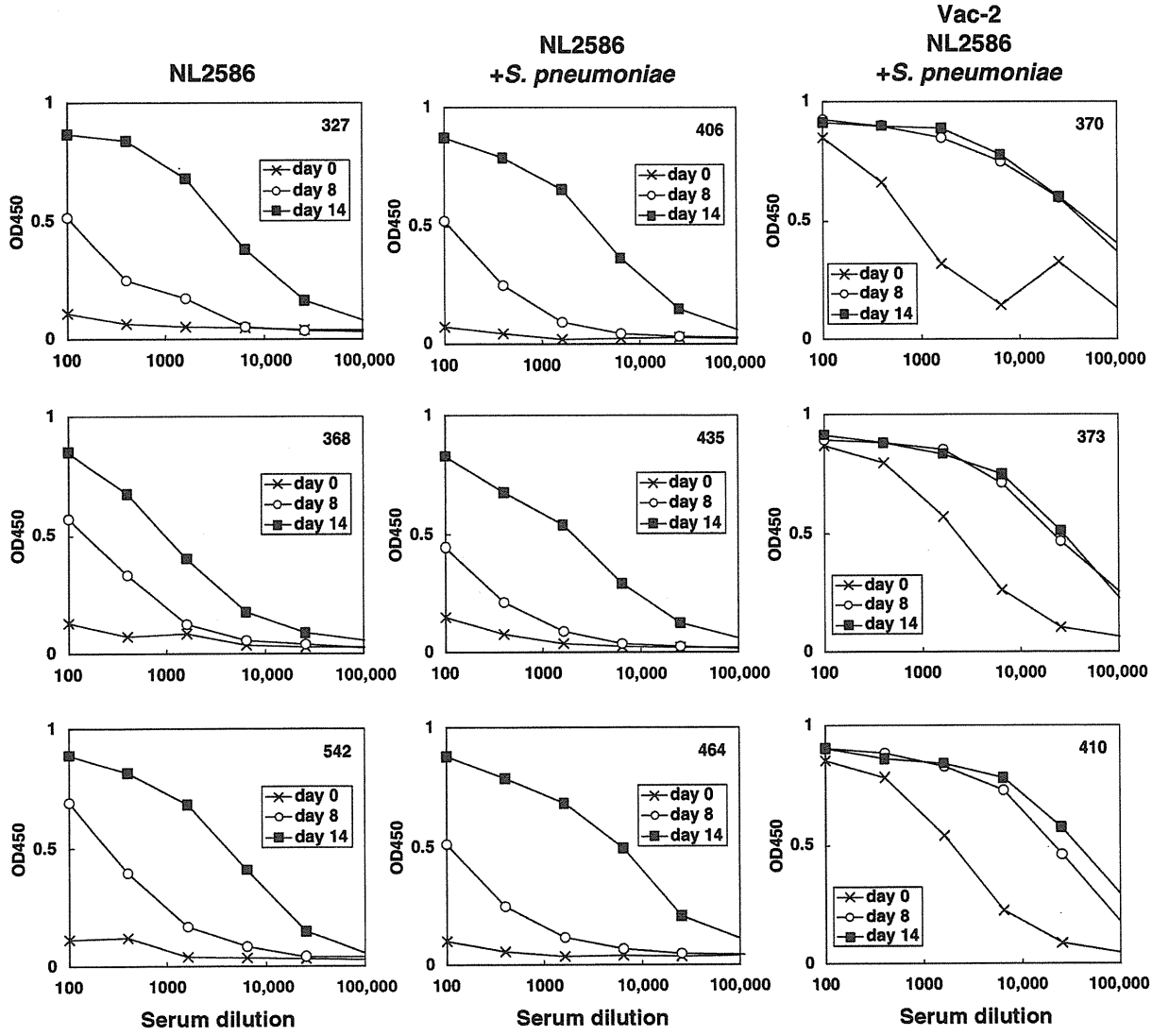

Fig. 6 Antibody responses specific for H7N7 vaccine antigens in cynomolgus macaques after challenge infection with NL2586. Sera were collected before (day 0) and after inoculation with NL2586 with or without *Streptococcus pneumoniae* (days 8 and 14). IgG antibodies specific for Vac-2 antigens in sera were analyzed at indicated dilutions as described in Fig. 2.

J Med Primatol **39** (2010) 58–70

Table 4 Neutralization activity of NL2586 with sera obtained after challenge with NL2586 and *Streptococcus pneumoniae*

Inoculation	Animal	50% neutralization titer (log 2)
NL2586	327	6.67
	368	5.50
	542	5.33
NL2586	406	5.17
+*S. pneumoniae*	435	4.00
	464	5.67
Vac-2	370	4.67
NL2586	373	5.83
+*S. pneumoniae*	410	6.23

Serum samples were collected 14 days after challenge infection with NL2586 with or without *S. pneumoniae*. The averages of 50% neutralization titers against NL2586 were 5.83, 4.95 and 5.58 in sera from macaques infected with NL2586 alone, macaques infected with NL2586 and *S. pneumoniae*, and macaques infected with NL2586 and *S. pneumoniae* after vaccination respectively. *P*-values with Student's *t*-test are >0.05 (NL2586 vs. NL2586 + *S. pneumoniae*, NL2586 vs. Vac-2 + NL286 + *S. pneumoniae*, and NL2586 + *S. pneumoniae* vs. Vac-2 + *S. pneumoniae*).

niae (Fig. 7, middle panels). A vaccinated macaque 370 showed higher increase in IgG specific for *S. pneumoniae* on day 8 than in that on day 14. This seems that immunological memory against *S. pneumoniae* has been present due to previous infection (Fig. 7, right panels). In two other vaccinated macaques (Nos 373 and 410), very weak or almost no IgG response was detected in sera. These findings suggest that viral replication may enhance IgG responses against *S. pneumoniae* in naïve animals, although IgG detected on day 14 was not sufficient to inhibit bacterial growth in the lungs (Table 2). Alternatively, as bacterial colonies in the vaccinated macaques were fewer than those in the unvaccinated macaques (Tables 1 and 2), IgG responses against *S. pneumoniae* might not be significant in the vaccinated macaques (Nos 373 and 410).

Discussion

Seasonal influenza virus infection occasionally induces secondary bacterial infection that results in substantial morbidity and mortality. Suppression of host immunity, including neutrophil function and macrophage-mediated microbial clearance [1, 4, 13, 24], and induction of inhibitory IL-10 [27, 28] are thought to be involved in the increased morbidity and mortality. It has not been determined whether mixed infection with HPAIV and bacteria causes more severe morbidity and higher mortality than infection with HPAIV alone, although co-infection with HPAIV and bacteria has not been detected in patients [5, 26]. Thus, in order to prevent severe morbidity and mortality in humans in future pandemics, it should be determined whether HPAIV infection with bacterial infection causes more severe morbidity than does HPAIV infection alone and whether regulation of HPAIV replication ameliorates bacterial pneumonia in experimental mixed infection using a macaque model as a preclinical study.

Some studies have shown that preceding influenza virus infection enhanced bacterial pneumonia with severe morbidity [6, 9, 11, 14]. Influenza viruses induce lung epithelial apoptosis via macrophage activation, resulting in the loss of defense capacity against bacteria in lung epithelia and the establishment of appropriate environment for bacterial growth [7]. Nonetheless, simultaneous infection with H7N7 HPAIV and *S. pneumoniae* in macaques did not induce severe pneumonia including diffuse alveolar damage at autopsy; only modest pneumonia immediately following lymphocyte infiltration was observed. Histology of the lungs of macaques simultaneously challenged with H7N7 HPAIV and *S. pneumoniae* indicated that the pneumonia seemed to be in a repairing phase with inflammatory cells infiltrating the alveoli being mainly lymphocytes with a few neutrophils, although pneumonia caused by *S. pneumoniae* occurred in addition to pneumonitis caused by H7N7 HPAIV, and pneumonia with neutrophils was not significant in lungs of macaques inoculated with NL2586 alone. As lung epithelial apoptosis via macrophage activation by influenza viruses seems to be responsible for severe pneumonia in co-infection, simultaneous infection but not preceding influenza viral infection might induce modest pneumonia. Alternatively, it is possible that pathogenicity of *S. pneumoniae* in macaques was low or *S. pneumoniae* growth might be regulated in some degree by host responses as *S. pneumoniae* might have been inoculated before desensitization of TLR by influenza virus infection in the simultaneous inoculation with HPAIV and *S. pneumonia* [4]. Further study should be required to reveal whether *S. pneumoniae* infection after HPAIV infection causes severe morbidity and mortality in a macaque model.

Vaccination against H7N7 HPAIV decreased morbidity caused by H7N7 HPAIV and *S. pneumoniae* in the macaques. Bacterial growth in the lungs was decreased by vaccination against H7N7 HPAIV, although the reduction in bacterial colonies was not statistically significant. Similarly, mitigation of the pneumonia was histologically observed in the lungs of vaccinated macaques. It is likely that the aforementioned lung epithelial apoptosis caused by influenza viruses is somehow involved in the enhancement

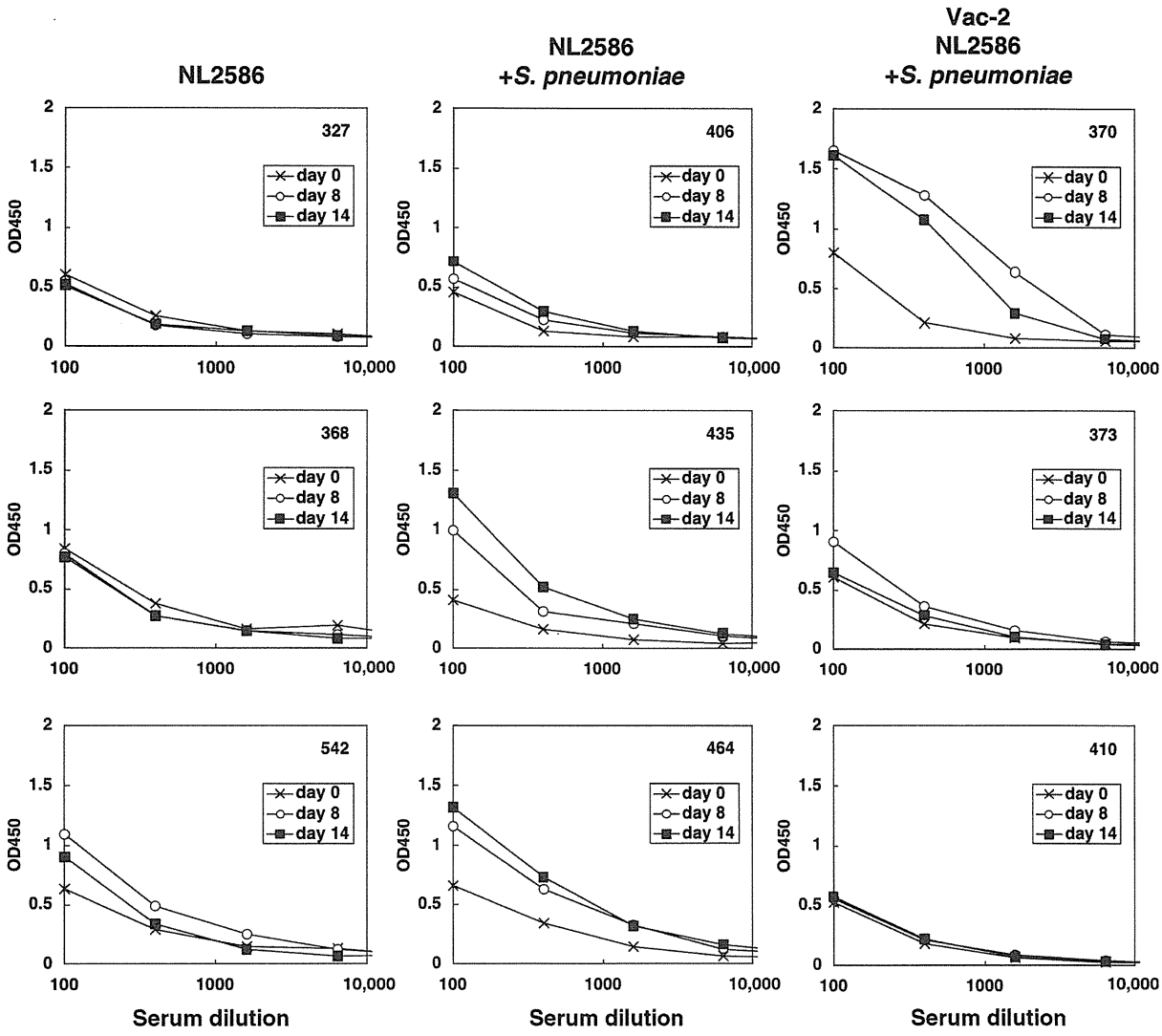

Fig. 7 Antibody responses specific for *Streptococcus pneumoniae* antigens in cynomolgus macaques after challenge infection with NL2586. Sera were collected before (day 0) and after inoculation of NL2586 with or without *S. pneumoniae* (days 8 and 14). IgG antibodies specific for *S. pneumonia* antigens in sera were analyzed at indicated dilutions as described in Fig. 2.

of bacterial pneumonia and that H7N7 HPAIV and *S. pneumoniae* interact with each other directly and indirectly in the development of pneumonia and pneumonitis.

In general, IL-10 expression is upregulated in influenza virus and *S. pneumoniae* infection of mice and IL-10 inhibits severe inflammatory responses in the lungs [12, 27, 28]. However, in the present study, *S. pneumoniae* infection suppressed IL-10 production, supporting histological findings and efficacy of antiviral vaccination. Furthermore, the reduction of IL-10 is assumed to finally induce cytokine storm after mixed infection with HPAIV and *S. pneumoniae* [3]. This assumption should be evidenced in near future.

Vaccination against HPAIV decreased the severity of pneumonia caused by bacterial superinfection, and prognosis of HPAIV-infected patients might be improved. Therefore, it might be crucial to prepare vaccines against future pandemic strains in order to prevent severe bacterial pneumonia as observed in the H1N1 pandemic in 1918 [10].

Acknowledgments

This study was supported by the Program of Founding Research Centers for Emerging and Reemerging Infectious Diseases, MEXT Japan. We thank Dr Ilaria Capua for providing NL2586, Dr Akira Yokoe for his

help in histological examinations, and Drs Kunio Ishibashi, Norio Okahara and Takahiro Nakagawa for animal care.

References

1 Abramson JS, Giebink GS, Mills EL, Quie PG: Polymorphonuclear leukocyte dysfunction during influenza virus infection in chinchillas. *J Infect Dis* 1981; **143**:836–45.

2 Brundage JF: Interactions between influenza and bacterial respiratory pathogens: implications for pandemic preparedness. *Lancet Infect Dis* 2006; **6**:303–12.

3 De Jong MD, Simmons CP, Thanh TT, Hien VM, Smith GJ, Chau TN, Hoang DM, Van Vinh Chau N, Khanh TH, Dong VC, Qui PT, Van Cam B, Ha DQ, Guan Y, Peiris JS, Chinh NT, Hien TT, Farrar J: Fatal outcome of human influenza A (H5N1) is associated with high viral load and hypercytokinemia. *Nat Med* 2006; **12**:1203–7.

4 Didierlaurent A, Goulding J, Patel S, Snelgrove R, Low L, Bebien M, Lawrence T, Van Rijt LS, Lambrecht BN, Sirard JC, Hussell T: Sustained desensitization to bacterial Toll-like receptor ligands after resolution of respiratory influenza infection. *J Exp Med* 2008; **205**:323–9.

5 Fouchier RA, Schneeberger PM, Rozendaal FW, Broekman JM, Kemink SA, Munster V, Kuiken T, Rimmelzwaan GF, Schutten M, Van Doornum GJ, Koch G, Bosman A, Koopmans M, Osterhaus AD: Avian influenza A virus (H7N7) associated with human conjunctivitis and a fatal case of acute respiratory distress syndrome. *Proc Natl Acad Sci U S A* 2004; **101**:1356–61.

6 Gupta RK, George R, Nguyen-Van-Tam JS: Bacterial pneumonia and pandemic influenza planning. *Emerg Infect Dis* 2008; **14**:1187–92.

7 Herold S, Steinmueller M, Von Wulffen W, Cakarova L, Pinto R, Pleschka S, Mack M, Kuziel WA, Corazza N, Brunner T, Seeger W, Lohmeyer J: Lung epithelial apoptosis in influenza virus pneumonia: the role of macrophage-expressed TNF-related apoptosis-inducing ligand. *J Exp Med* 2008; **205**:3065–77.

8 Itoh Y, Ozaki H, Tsuchiya H, Okamoto K, Torii R, Sakoda Y, Kawaoka Y, Ogasawara K, Kida H: A vaccine prepared from a non-pathogenic H5N1 avian influenza virus strain confers protective immunity against highly pathogenic avian influenza virus infection in cynomolgus macaques. *Vaccine* 2008; **26**:562–72.

9 Jennings LC, Anderson TP, Beynon KA, Chua A, Laing RT, Werno AM, Young SA, Chambers ST, Murdoch DR: Incidence and characteristics of viral community-acquired pneumonia in adults. *Thorax* 2008; **63**:42–8.

10 Kida H, Sakoda Y: Library of influenza virus strains for vaccine and diagnostic use against highly pathogenic avian influenza and human pandemics. *Dev Biol (Basel)* 2006; **124**:69–72.

11 Madhi SA, Klugman KP: A role for *Streptococcus pneumoniae* in virus-associated pneumonia. *Nat Med* 2004; **10**:811–3.

12 Mckinstry KK, Strutt TM, Buck A, Curtis JD, Dibble JP, Huston G, Tighe M, Hamada H, Sell S, Dutton RW, Swain SL: IL-10 deficiency unleashes an influenza-specific Th17 response and enhances survival against high-dose challenge. *J Immunol* 2009; **182**:7353–63.

13 Mcnamee LA, Harmsen AG: Both influenza-induced neutrophil dysfunction and neutrophil-independent mechanisms contribute to increased susceptibility to a secondary *Streptococcus pneumoniae* infection. *Infect Immun* 2006; **74**:6707–21.

14 Morens DM, Taubenberger JK, Fauci AS: Predominant role of bacterial pneumonia as a cause of death in pandemic influenza: implications for pandemic influenza preparedness. *J Infect Dis* 2008; **198**:962–70.

15 Page KR, Scott AL, Manabe YC: The expanding realm of heterologous immunity: friend or foe? *Cell Microbiol* 2006; **8**:185–96.

16 Philipp MT, Purcell JE, Martin DS, Buck WR, Plauche GB, Ribka EP, Denoel P, Hermand P, Leiva LE, Bagby GJ, Nelson S: Experimental infection of rhesus macaques with *Streptococcus pneumoniae*: a possible model for vaccine assessment. *J Med Primatol* 2006; **35**:113–22.

17 Sakabe S, Sakoda Y, Haraguchi Y, Isoda N, Soda K, Takakuwa H, Saijo K, Sawata A, Kume K, Hagiwara J, Tuchiya K, Lin Z, Sakamoto R, Imamura T, Sasaki T, Kokumai N, Kawaoka Y, Kida H: A vaccine prepared from a non-pathogenic H7N7 virus isolated from natural reservoir conferred protective immunity against the challenge with lethal dose of highly pathogenic avian influenza virus in chickens. *Vaccine* 2008; **26**:2127–34.

18 Sawai T, Itoh Y, Ozaki H, Isoda N, Okamoto K, Kashima Y, Kawaoka Y, Takeuchi Y, Kida H, Ogasawara K: Induction of cytotoxic T-lymphocyte and antibody responses against highly pathogenic avian influenza virus infection in mice by inoculation of apathogenic H5N1 influenza virus particles inactivated with formalin. *Immunology* 2008; **124**:155–65.

19 Seki M, Higashiyama Y, Tomono K, Yanagihara K, Ohno H, Kaneko Y, Izumikawa K, Miyazaki Y, Hirakata Y, Mizuta Y, Tashiro T, Kohno S: Acute infection with influenza virus enhances susceptibility to fatal pneumonia following *Streptococcus pneumoniae* infection in mice with chronic pulmonary colonization with Pseudomonas aeruginosa. *Clin Exp Immunol* 2004; **137**:35–40.

20 Soda K, Sakoda Y, Isoda N, Kajihara M, Haraguchi Y, Shibuya H, Yoshida H, Sasaki T, Sakamoto R, Saijo K,

Hagiwara J, Kida H: Development of vaccine strains of H5 and H7 influenza viruses. *Jpn J Vet Res* 2008; **55**:93–8.
21 Stiver HG: The threat and prospects for control of an influenza pandemic. *Expert Rev Vaccines* 2004; **3**:35–42.
22 Sugasawara RJ, Prato CM, Sippel JE: Enzyme-linked immunosorbent assay with a monoclonal antibody for detecting group A meningococcal antigens in cerebrospinal fluid. *J Clin Microbiol* 1984; **19**:230–4.
23 Sun J, Madan R, Karp CL, Braciale TJ: Effector T cells control lung inflammation during acute influenza virus infection by producing IL-10. *Nat Med* 2009; **15**:277–84.
24 Sun K, Metzger DW: Inhibition of pulmonary antibacterial defense by interferon-γ during recovery from influenza infection. *Nat Med* 2008; **14**:558–64.
25 Thomas MJ, Flanary LR, Brown BA, Katze MG, Baskin CR: Use of human nasal cannulas during bronchoscopy procedures as a simple method for maintaining adequate oxygen saturation in pigtailed macaques (*Macaca nemestrina*). *J Am Assoc Lab Anim Sci* 2006; **45**:44–8.
26 Tran TH, Nguyen TL, Nguyen TD, Luong TS, Pham PM, Nguyen VC, Pham TS, Vo CD, Le TQ, Ngo TT, Dao BK, Le PP, Nguyen TT, Hoang TL, Cao VT, Le TG, Nguyen DT, Le HN, Nguyen KT, Le HS, Le VT, Christiane D, Tran TT, Menno De J, Schultsz C, Cheng P, Lim W, Horby P, Farrar J: World Health Organization International Avian Influenza Investigative Team: Avian influenza A (H5N1) in 10 patients in Vietnam. *N Engl J Med* 2004; **350**:1179–88.
27 Van Der Sluijs KF, Nijhuis M, Levels JH, Florquin S, Mellor AL, Jansen HM, Van Der Poll T, Lutter R: Influenza-induced expression of indoleamine 2,3-dioxygenase enhances interleukin-10 production and bacterial outgrowth during secondary pneumococcal pneumonia. *J Infect Dis* 2006; **193**:214–22.
28 Van Der Sluijs KF, Van Elden LJ, Nijhuis M, Schuurman R, Pater JM, Florquin S, Goldman M, Jansen HM, Lutter R, Van Der Poll T: IL-10 is an important mediator of the enhanced susceptibility to pneumococcal pneumonia after influenza infection. *J Immunol* 2004; **172**:7603–9.
29 Walzl G, Tafuro S, Moss P, Openshaw PJ, Hussell T: Influenza virus lung infection protects from respiratory syncytial virus-induced immunopathology. *J Exp Med* 2000; **192**:1317–26.

J Med Primatol **39** (2010) 58–70

OPEN ACCESS Freely available online

PLoS one

Predicting the Antigenic Structure of the Pandemic (H1N1) 2009 Influenza Virus Hemagglutinin

Manabu Igarashi[1], Kimihito Ito[1], Reiko Yoshida[1], Daisuke Tomabechi[1], Hiroshi Kida[1,2,3], Ayato Takada[1]*

1 Department of Global Epidemiology, Hokkaido University Research Center for Zoonosis Control, Sapporo, Japan, **2** Department of Disease Control, Graduate School of Veterinary Medicine, Hokkaido University, Sapporo, Japan, **3** OIE Reference Laboratory for Highly Pathogenic Avian Influenza, Sapporo, Japan

Abstract

The pandemic influenza virus (2009 H1N1) was recently introduced into the human population. The hemagglutinin (HA) gene of 2009 H1N1 is derived from "classical swine H1N1" virus, which likely shares a common ancestor with the human H1N1 virus that caused the pandemic in 1918, whose descendant viruses are still circulating in the human population with highly altered antigenicity of HA. However, information on the structural basis to compare the HA antigenicity among 2009 H1N1, the 1918 pandemic, and seasonal human H1N1 viruses has been lacking. By homology modeling of the HA structure, here we show that HAs of 2009 H1N1 and the 1918 pandemic virus share a significant number of amino acid residues in known antigenic sites, suggesting the existence of common epitopes for neutralizing antibodies cross-reactive to both HAs. It was noted that the early human H1N1 viruses isolated in the 1930s–1940s still harbored some of the original epitopes that are also found in 2009 H1N1. Interestingly, while 2009 H1N1 HA lacks the multiple *N*-glycosylations that have been found to be associated with an antigenic change of the human H1N1 virus during the early epidemic of this virus, 2009 H1N1 HA still retains unique three-codon motifs, some of which became *N*-glycosylation sites via a single nucleotide mutation in the human H1N1 virus. We thus hypothesize that the 2009 H1N1 HA antigenic sites involving the conserved amino acids will soon be targeted by antibody-mediated selection pressure in humans. Indeed, amino acid substitutions predicted here are occurring in the recent 2009 H1N1 variants. The present study suggests that antibodies elicited by natural infection with the 1918 pandemic or its early descendant viruses play a role in specific immunity against 2009 H1N1, and provides an insight into future likely antigenic changes in the evolutionary process of 2009 H1N1 in the human population.

Citation: Igarashi M, Ito K, Yoshida R, Tomabechi D, Kida H, et al. (2010) Predicting the Antigenic Structure of the Pandemic (H1N1) 2009 Influenza Virus Hemagglutinin. PLoS ONE 5(1): e8553. doi:10.1371/journal.pone.0008553

Editor: Robert Belshaw, University of Oxford, United Kingdom

Received August 25, 2009; **Accepted** December 4, 2009; **Published** January 1, 2010

Funding: This work was supported by Grants-in-Aid for Scientific Research (B) (19300041) from the Japan Society for the Promotion of Science (JSPS), and for Young Scientists (B) (21780272) from the Ministry of Education, Culture, Sports, Science and Technology (MEXT), Japan (http://www.mext.go.jp/english/index.htm), and in part, by the Program of Founding Research Centers for Emerging and Reemerging Infectious Diseases (05021011) from MEXT, Japan. The funders had no role in study design, data collection and analysis, decision to publish, or preparation of the manuscript.

Competing Interests: The authors have declared that no competing interests exist.

* E-mail: atakada@czc.hokudai.ac.jp

Introduction

In April 2009, pandemic (H1N1) 2009 influenza virus (2009 H1N1) was first found in patients with febrile respiratory illness in the United States and Mexico, and has spread rapidly across the world by human-to-human transmission. On the 11th of June 2009, the World Health Organization declared a global pandemic of 2009 H1N1 infection. H1N1 influenza virus caused a pandemic in 1918 (1918 H1N1) [1], and its descendant virus with highly altered antigenicity of the viral surface protein, hemagglutinin (HA) has been causing "seasonal flu" in humans.

The 2009 H1N1 resulted from genetic reassortment between the recently circulating swine H1 viruses in North America and the avian-like swine viruses in Europe [2]. Phylogenetic analysis showed that the HA gene of 2009 H1N1 was derived from the so-called "classical swine H1N1" virus, which likely shares a common ancestor with the recent human H1N1 virus [2]. Accordingly, it has been reported that the early strains of the classical swine H1N1 virus, which was first identified in North America in 1930, were antigenically similar to the prototype strain of 1918 H1N1, A/South Carolina/1/1918 (SC1918), detected from a few victims of the pandemic in 1918 [3,4]. Since antigenic changes occur more slowly in swine than in the human population [5], HA of the classical swine H1N1 virus was antigenically highly conserved until the late 1990s [4,6], raising the possibility that the recently emerged 2009 H1N1 may still retain an antigenic structure similar to that of SC1918 and the early isolates of its descendants.

In this study, we generated three-dimensional (3D) structures of the HA molecules of 1918 H1N1, its descendent, recent seasonal H1N1 viruses, and 2009 H1N1, and compared their antigenic structures to look for evidence for the existence of shared epitopes for neutralizing antibodies. Since the 2009 H1N1 HA antigenic sites will be targeted by antibody-mediated selection pressure in humans in the near future, we further discuss possible directions of antigenic changes in the evolutionary process of this pandemic virus.

Results and Discussion

It is known that the H1 HA molecules have four distinct antigenic sites: Sa, Sb, Ca, and Cb [7,8,9,10] (Figure 1). As a result, these sites consist of the most variable amino acids in the HA molecule of the seasonal human H1N1 viruses that have been subjected to antibody-mediated immune pressure since its

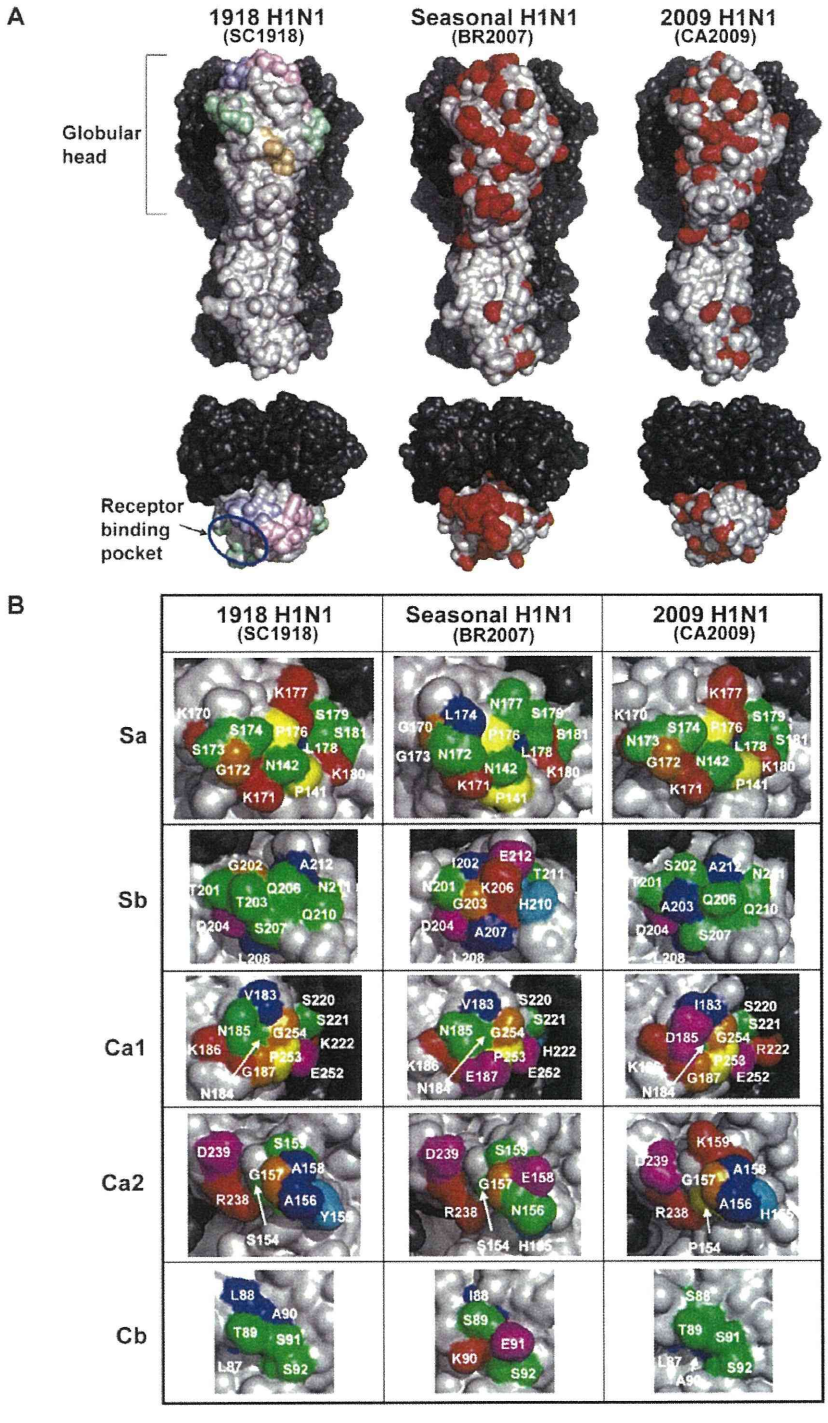

Figure 1. Comparison of the structures of antigenic sites on the HA molecules among 1918 H1N1 (SC1918), recent seasonal H1N1 (BR2007), and 2009 H1N1 (CA2009). Three-dimensional models of the H1 HA molecules of SC1918, BR2007, and CA2009 were constructed based on the HA crystal structures of A/South Carolina/1/18, A/Puerto Rico/8/34, and A/swine/Iowa/30, respectively (PDB codes: 1RUZ, 1RU7, and 1RUY, respectively). Models with solvent-accessible surface representation were generated by a molecular modeling method as described in the Methods section. Molecular surface of the HA trimers viewed on its side (upper) and top (lower) are shown (A). One monomer (center) is colored gray and the others are colored dark gray. The antigenic sites, Sa (light pink), Sb (light blue), Ca (pale green), and Cb (light orange) are indicated on the model of SC1918 HA. The spatial locations of amino acid residues that are distinct from those of SC1918 HA are shown in red on the models of BR2007 and CA2009 HAs. Each amino acid residue is mapped on the close-up views of each antigenic site of SC1918, BR2007, and CA2009 HAs (B). The Ca site is divided into subregions, Ca1 and Ca2. Amino acids are colored by the default ClustalX color scheme [29]: Trp, Leu, Val, Ile, Met, Phe, and Ala (blue); Lys and Arg (red); Thr, Ser, Asn, and Gln (green); Cys (pink); Asp and Glu (magenta); Gly (orange); His and Tyr (cyan); Pro (yellow).
doi:10.1371/journal.pone.0008553.g001

Table 1. Amino acid similarity in the HA antigenic sites among recent seasonal H1N1 (BR2007), 2009 H1N1 (CA2009), and 1918 H1N1 (SC1918).

Antigenic sites	No. amino acids involved	No. of amino acids identical to SC1918	
		BR2007	CA2009
Sa	13	8	12
Sb	12	4	10
Ca	19	13	13
Cb	6	2	5

doi:10.1371/journal.pone.0008553.t001

emergence in 1918 [3]. To investigate the structures of these antigenic sites of 2009 H1N1, 3D structures of the HA molecules of SC1918, the recent seasonal human H1N1 virus A/Brisbane/59/2007 (BR2007), and 2009 H1N1 A/California/04/2009 (CA2009) [2] were constructed by a homology modeling approach, and compared by mapping all the amino acid residues that were distinct from those of SC1918 HA (Figure 1 and Table S1). We found that most of these antigenic sites of BR2007 HA predominantly contained altered amino acid residues if compared with SC1918. By contrast, amino acid residues at these positions were relatively conserved in CA2009 HA. Notably, the Sa and Sb sites that contain many amino acids involved in neutralizing epitopes near the receptor binding pockets [8,10] remain almost intact in CA2009 HA (Table 1), suggesting that antibodies raised by natural infection with SC1918 or its antigenically related descendant viruses play a role in specific immunity against CA2009.

We then constructed 3D structures of the representative strains of seasonal H1 viruses that had been isolated since 1934, and tracked the amino acid substitutions on their HA molecules (Figure 2 and Figure S1). We confirmed that amino acid substitutions associated with the antigenic changes gradually accumulated on the globular head region of HA and were distributed over four distinct antigenic sites. However, it was noted that the early isolates represented by the A/Puerto Rico/8/1934 and A/Bellamy/1942 strains, but not the strains isolated after the

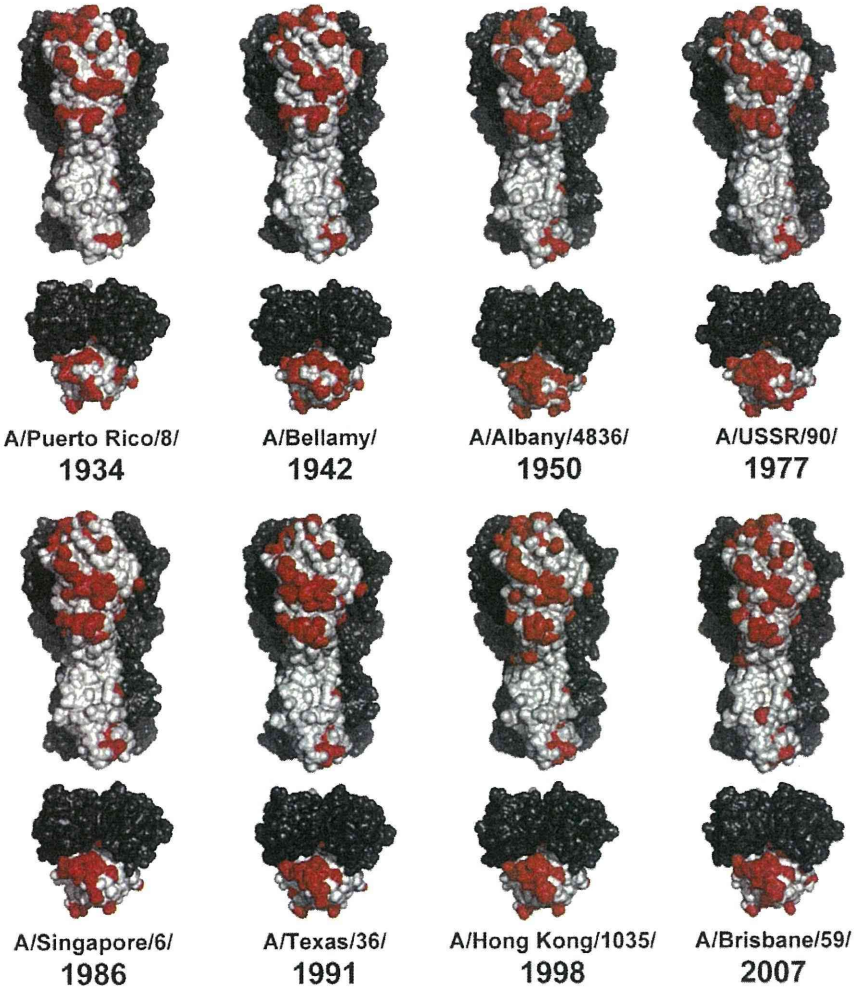

Figure 2. Amino acid substitutions associated with antigenic changes of seasonal human H1N1 virus HAs. All models were generated and shown by a molecular modeling method as described in the Methods section and the legend of Figure 1.
doi:10.1371/journal.pone.0008553.g002

1950s, still harbored unchanged amino acids forming potential neutralizing epitopes in the Sa and Sb sites (Figure 2). It seems likely that most of the amino acids on these antigenic sites were eventually substituted in the late 1940s (Figure S1).

It is well-documented that antigenic changes of HA occasionally result in the acquisition of carbohydrate side chains on the HA molecule [8,11]. Since the carbohydrate side chains in the vicinity of antigenic sites mask the neutralizing epitopes on the HA surface, amino acid substitutions associated with acquisition of carbohydrate chains are believed to efficiently generate antigenic variants. Accordingly, recent seasonal H1N1 viruses have acquired 4–5 *N*-glycosylation sites (Asn-Xaa-Ser/Thr, where Xaa is any amino acid except Pro) in the globular head region of HA [12,13], whereas SC1918 HA had only one site, at Asn 104 (Figure 3).

Interestingly, CA2009 also has a single potential *N*-glycosylation site at the same position in the globular head region of HA (Figure 3), despite the fact that the classical swine H1N1 virus emerged in the early 1900s and was circulating in the pig population until recently. This prompted us to estimate the potential of 2009 H1N1 to acquire additional *N*-glycosylation sites on its HA, which may be related to its future evolutionary process in the human population. We previously defined a three-codon motif that becomes an *N*-glycosylation site with a single-nucleotide mutation as "*Cand1*", and suggested that the presence of the *Cand1* sites in the HA sequence is one of the key factors for human influenza A viruses to rapidly acquire *N*-glycosylation sites during the early epidmic in the human population [13]. We compared the number of the *Cand1* sites in the HA globular head region between SC1918 and CA2009 (Figure 3 and Table S1). We found that CA2009 HA possessed three *Cand1* sites on the antigenic sites Sa and Ca, all of which were also present at the same position in SC1918 HA (positions of the first Asn residue, 177, 179, and 184). Of these, the *Cand1* sites with positions at 177 and 179 had actually become potential *N*-glycosylation sites in human H1N1 viruses, although these two sites did not exist concurrently [12]. It is noted that these two *Cand1* sites are still present on the surface of CA2009 HA, suggesting the likelihood of additional *N*-glycosylation at these sites during future antigenic changes of 2009 H1N1 HA.

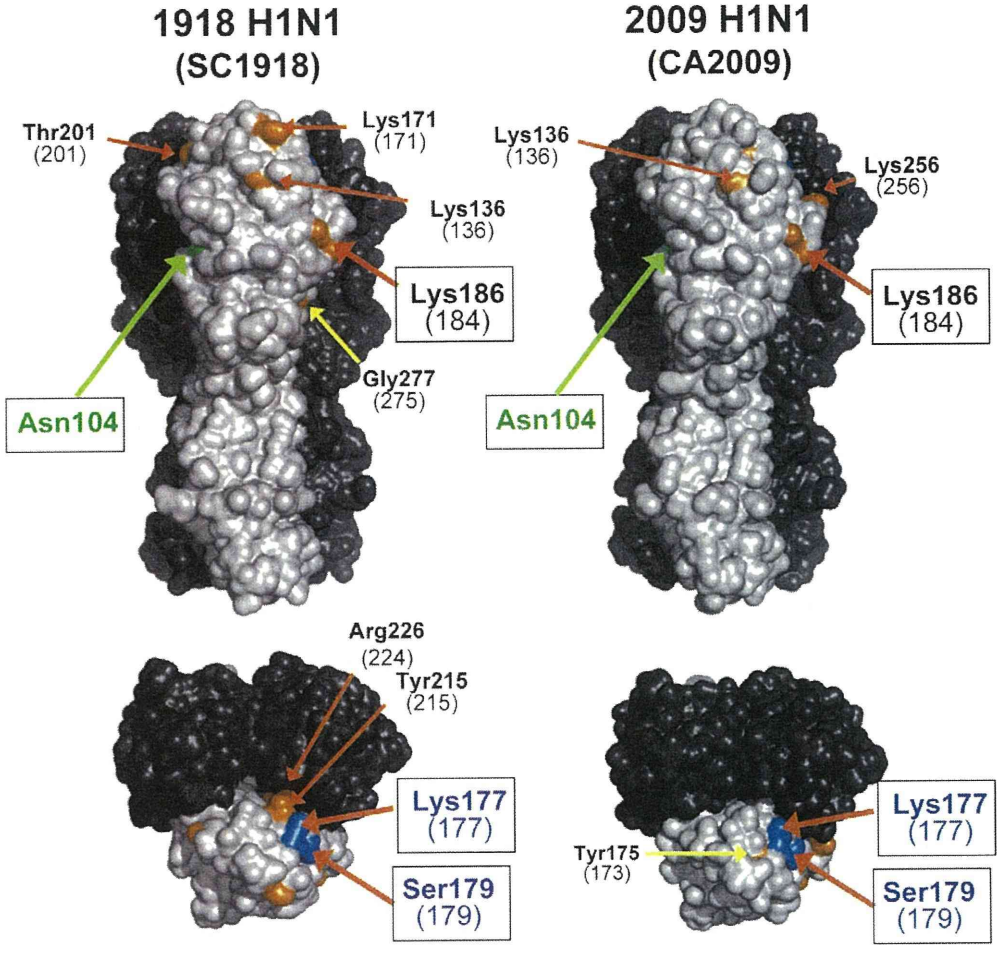

Figure 3. Comparison of the *N*-glycosylation potential of HA between SC1918 and CA2009. Residues shown in green represent Asn at the actually existing *N*-glycosylation sites. Residues shown in orange or blue represent the amino acids in *Cand1* sites that require a nucleotide substitution to produce *N*-glycosylation sites. Residues shown in blue represent the amino acids that were actually substituted, resulting in the acquisition of *N*-glycosylation sites during the antigenic evolution of human H1N1 viruses. Numbers in parentheses show the positions of Asn residues that may be linked to carbohydrate chains, if respective *Cand1* sites mutate to have *N*-glycosylation sites. All models were generated as described in the Methods section and the legend of Figure 1.
doi:10.1371/journal.pone.0008553.g003

In this paper, we employed 3D structures constructed by a homology modeling method to map amino acid residues on the antigenic sites of HA. When compared to the presentation of simple primary sequences, the 3D presentation has following advantages: (a) There are several amino acid residues that are buried beneath the surface of the HA molecule, even if they are included in the antigenic sites described by the primary amino acid sequences. Since such amino acid residues do not directly contribute to the interaction with antibodies, the surface structures of antigenic sites that are accessible for antibodies can be compared more precisely in the presentation by 3D models than by the primary amino acid sequence. (b) An epitope likely consists of multiple amino acid residues belonging to different antigenic regions presented by the primary amino acid sequence. Such conformational epitopes can be illustrated only by the 3D presentation. (c) One of the purposes of this study is to provide a structural basis to confirm antigenic similarity between the 1918 H1N1 and the pandemic 2009 H1N1 viruses. For this purpose, we employed a homology modeling method rather than simply mapping on the existing crystal structure (e.g. 1918 H1N1 HA), since this method is generally used to generate a 3D structure of a protein molecule if there is no available crystal structure of the target protein [14]. Thus, we believe that this method produces more likely HA structure models of the viruses whose HA crystal structure are not available (e.g. CA2009). In fact, our homology modeling approach suggests that several amino acid residues were occasionally buried beneath or exposed to the surface of HA molecule, depending on the substitutions found in the viruses examined (Figure 1B and Figure S1). The homology modeling approach might enable us to analyze such dynamics of antigenic changes at molecular levels.

Our analysis indicated that 2009 H1N1 had undergone less significant antigenic changes of HA in the pig population than human H1N1 virus since their emergence in the early 1900s. The Centers for Disease Control and Prevention reported that vaccination with recent (2005–2009) human H1N1 viruses was unlikely to provide protection against 2009 H1N1 [15]; however, cross-reactive antibodies were detected in 33% of people aged 60 and over. Another report showed that appreciable neutralizing antibodies against CA2009 were present in the sera collected from individuals born before 1918 [16]. Our 3D models provide a protein-structural basis supporting these observations, and further suggest that infection with the 1918 H1N1 or early human H1N1 viruses (viruses present before the 1940s), but not with antigenically divergent human H1N1 viruses circulating after the 1950s, elicited cross-neutralizing antibodies to 2009 H1N1.

This virus will soon be subjected to complex immunological selection pressure by the antibody response that will be induced in the human population by vaccination and/or natural infection with homologous viruses, and pre-existing immunity cross-reactive to the early descendants of 1918 H1N1. In the present study, we showed that the antigenic structure of 2009 H1N1 HA might still be similar, at least in part, to that of the 1918 H1N1 HA. We speculate that the 2009 H1N1 HA antigenic sites involving the conserved amino acids will soon be targeted by neutralizing antibodies in humans. Thus, it is of interest to monitor whether these antigenic sites of 2009 H1N1 will undergo similar patterns of amino acid substitutions to those seen in seasonal H1N1 viruses during its epidemic period (Figure 4). Interestingly, we found that some of the recent variants of the 2009 H1N1 virus (as of November 3, 2009) have indeed undergone substitutions identical to those predicted in Figure 4. Although the present study still needs to be supported by experimental data, our approach may provide new perspectives on collective immunity against 2009 H1N1 and an insight into future antigenic changes of this new human pandemic influenza virus.

Methods

Sequence Data of HA Genes

Nucleotide sequences for HA genes of SC1918 (AF117241), BR2007 (CY030230), CA2009 (FJ966082), A/Puerto Rico/8/1934/Mount Sinai (AF389118), A/Bellamy/1942 (CY009276), A/Albany/4836/1950 (CY021701), A/USSR/90/1977 (DQ508897), A/Singapore/6/1986 (CY020477), A/Texas/36/1991 (AY289927), and A/Hong Kong/1035/1998 (AF386777) [2,3,17,18,19,20] were obtained from Influenza Virus Resource at the National Center for Biotechnology Information (NCBI) (http://www.ncbi.nlm.nih.gov/genomes/FLU/FLU.html).

Molecular Modeling

MODELLER 9v6 [21] was used for homology modeling of HA structures. After one hundred models of the HA trimer were generated, the model was chosen by a combination of the MODELLER objective function value and the discrete optimized protein energy (DOPE) statistical potential score [22]. After addition of hydrogen atoms, the model was refined by energy minimization (EM) with the minimization protocols in the Discovery Studio 2.1 software package (Accelrys, San Diego, CA) using a CHARMm force field. Steepest descent followed by conjugate gradient minimizations was carried out until the root mean square (rms) gradient was less than or equal to 0.01 kcal/mol/Å. The generalized Born implicit solvent model [23,24] was used to model the effects of solvation. The HA model was finally evaluated by using PROCHECK [25], WHATCHECK [26], and VERIFY-3D [27]. All figures are shown as a solvent-accessible surface representation prepared by PyMOL (DeLano Scientific LLC) [28]. All HA structures constructed by a homology modeling method are available in Supplementary Files S1, S2, S3, S4, S5, S6, S7, and S8.

Sequence Data Analyses for *N*-Glycosylation Sites

Custom-made programs were developed with the Ruby language and used for investigating the numbers of potential *N*-glycosylation sites and candidate codons (*Cand1*) in HA sequences. The programs are available upon request.

Supporting Information

Table S1
Found at: doi:10.1371/journal.pone.0008553.s001 (0.04 MB PDF)

Figure S1 Amino acid substitutions of seasonal human H1N1 virus HAs shown in close-up views of each antigenic site. The strains used in this analysis are corresponding to those shown in Figure 2. Amino acids are colored according to the scheme in the legend of Figure 1B.
Found at: doi:10.1371/journal.pone.0008553.s002 (1.02 MB PDF)

File S1 PDB file of the homology model of H1 HA (A/California/04/2009) after energy minimizations.
Found at: doi:10.1371/journal.pone.0008553.s003 (0.20 MB ZIP)

File S2 PDB file of the homology model of H1 HA (A/Bellamy/1942) after energy minimizations.
Found at: doi:10.1371/journal.pone.0008553.s004 (0.20 MB ZIP)

File S3 PDB file of the homology model of H1 HA (A/Albany/4836/1950) after energy minimizations.

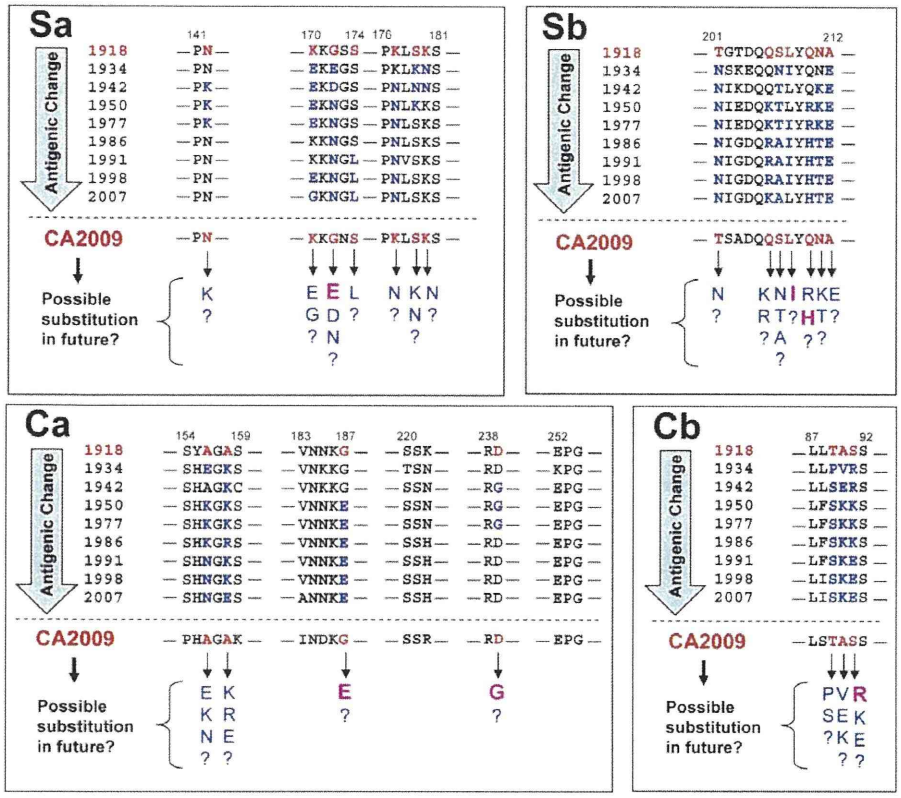

Figure 4. Prediction of the future amino acid substitutions on the antigenic sites of 2009 H1N1 HA. Amino acid sequences of HA antigenic sites of human H1N1 viruses are shown. Sequence data are corresponding to those of virus strains shown in Figures 1 and 2. Amino acid residues shared between 1918 H1N1 (SC1918) and 2009 H1N1 (CA2009) are shown in red, and those that have been substituted since 1934 are shown in blue. Amino acid residues indicated by arrows represent the predicted substitutions which might be associated with antigenic changes of 2009 H1N1 in the near future. The amino acid substitutions which have already been found in the recent variants of the 2009 H1N1 virus (as of November 3, 2009) are shown in bold pink letters.
doi:10.1371/journal.pone.0008553.g004

Found at: doi:10.1371/journal.pone.0008553.s005 (0.20 MB ZIP)

File S4 PDB file of the homology model of H1 HA (A/USSR/90/1977) after energy minimizations.
Found at: doi:10.1371/journal.pone.0008553.s006 (0.20 MB ZIP)

File S5 PDB file of the homology model of H1 HA (A/Singapore/6/1986) after energy minimizations.
Found at: doi:10.1371/journal.pone.0008553.s007 (0.20 MB ZIP)

File S6 PDB file of the homology model of H1 HA (A/Texas/36/1991) after energy minimizations.
Found at: doi:10.1371/journal.pone.0008553.s008 (0.20 MB ZIP)

File S7 PDB file of the homology model of H1 HA (A/Hong Kong/1035/1998) after energy minimizations.
Found at: doi:10.1371/journal.pone.0008553.s009 (0.20 MB ZIP)

File S8 PDB file of the homology model of H1 HA (A/Brisbane/59/2007) after energy minimizations.
Found at: doi:10.1371/journal.pone.0008553.s010 (0.20 MB ZIP)

Acknowledgments

We thank Teiji Murakami for excellent technical assistance and Kim Barrymore for editing the manuscript.

Author Contributions

Conceived and designed the experiments: MI KI HK AT. Analyzed the data: MI RY DT. Wrote the paper: MI AT.

References

1. Reid AH, Taubenberger JK (2003) The origin of the 1918 pandemic influenza virus: a continuing enigma. J Gen Virol 84: 2285–2292.
2. Garten RJ, Davis CT, Russell CA, Shu B, Lindstrom S, et al. (2009) Antigenic and genetic characteristics of swine-origin 2009 A(H1N1) influenza viruses circulating in humans. Science 325: 197–201.
3. Reid AH, Fanning TG, Hultin JV, Taubenberger JK (1999) Origin and evolution of the 1918 "Spanish" influenza virus hemagglutinin gene. Proc Natl Acad Sci U S A 96: 1651–1656.
4. Vincent AL, Lager KM, Ma W, Lekcharoensuk P, Gramer MR, et al. (2006) Evaluation of hemagglutinin subtype 1 swine influenza viruses from the United States. Vet Microbiol 118: 212–222.
5. Sugita S, Yoshioka Y, Itamura S, Kanegae Y, Oguchi K, et al. (1991) Molecular evolution of hemagglutinin genes of H1N1 swine and human influenza A viruses. J Mol Evol 32: 16–23.
6. Sheerar MG, Easterday BC, Hinshaw VS (1989) Antigenic conservation of H1N1 swine influenza viruses. J Gen Virol 70(Pt 12): 3297–3303.
7. Luoh SM, McGregor MW, Hinshaw VS (1992) Hemagglutinin mutations related to antigenic variation in H1 swine influenza viruses. J Virol 66: 1066–1073.
8. Caton AJ, Brownlee GG, Yewdell JW, Gerhard W (1982) The antigenic structure of the influenza virus A/PR/8/34 hemagglutinin (H1 subtype). Cell 31: 417–427.